

Cite this: *RSC Adv.*, 2017, 7, 21124

Received 6th February 2017

Accepted 29th March 2017

DOI: 10.1039/c7ra01530e

rsc.li/rsc-advances

## Formation of C<sub>60</sub> fullerene-bonded-CNTs using radio frequency plasma†

Shengxia Duan,<sup>ab</sup> Xia Liu,<sup>ab</sup> Yanan Wang,<sup>ab</sup> Dadong Shao,<sup>a</sup> Yuedong Meng,<sup>a</sup> Tasawar Hayat,<sup>de</sup> Ahmed Alsaedi<sup>d</sup> and Jiaxing Li<sup>id</sup>\*<sup>acd</sup>

C<sub>60</sub> fullerene-bonded-CNTs (CNBs) were successfully synthesized by radio frequency plasma (RF plasma) treatment for the first time. High-resolution transmission electron microscopy (HRTEM) and Raman spectroscopy were used to confirm the formation of the CNB structure. A possible mechanism was also proposed to explain the formation of CNBs. This RF plasma treatment may inspire a novel method to potentially overcome the synthetic difficulty of CNBs.

Hybrid carbon nanostructures integrating 0-dimensional (0D) fullerenes, 1D carbon nanotubes (CNTs), and 2D graphene can afford a compelling possibility to combine the great characteristics of individual carbon nano-allotropes in a selective manner.<sup>1</sup> The first hybrid carbon material, named the carbon nano-peapod, was discovered in 1998 by Smith *et al.*,<sup>2</sup> in which the fullerene molecules are encapsulated in CNTs (a schematic representation of the carbon nano-peapod is shown in Fig. S1†). After that, great contributions have been made to investigating the formation of carbon nano-peapods.<sup>3,4</sup> For instance, Luzzi *et al.* synthesized carbon nano-peapods from single-walled and double-walled nanotubes grown by a chemical vapor deposition (CVD) method.<sup>3</sup> Shen also utilized the molecular dynamics (MD) method to simulate the compression and tension of the carbon nano-peapod.<sup>4</sup> Besides carbon nano-peapod materials, carbon nanobuds (CNBs), a novel fullerene–CNT hybrid nanostructure, formed by fullerene units covalently attached to CNTs, have attracted increasing attention both experimentally and theoretically. Typically, nanobuds have been prepared by aerosol (floating catalyst) CVD method based on CO decomposition on iron particles produced from ferrocene vapour, shown in Scheme S1.†<sup>5</sup> The first experimentally obtained CNBs was reported by Kauppinen *et al.* via a ferrocene vapour decomposition.<sup>6</sup> The presence of C<sub>20</sub>, C<sub>42</sub> and C<sub>60</sub> fullerene units covalently bonded to the outer surface of the CNTs. The obtained CNBs exhibited enhanced cold electron field-emission properties.<sup>6</sup> Nicholls *et al.* also synthesized CNBs through a CVD

method and indicated that CNBs can be utilized as a precursor in the synthetic process of nanotube junction.<sup>7</sup> In addition to experimental studies, theoretical studies based on density functional theory (DFT) method were also carried out to investigate the properties of CNBs in various aspects,<sup>8</sup> such as its relative reactivity towards amine nucleophile<sup>8d</sup> and its Raman features of the CNBs.<sup>8e</sup>

The strong covalent bonding between fullerenes and CNTs in CNBs could provide the advantageous properties to this hybrid material that are unavailable for nano-peapods, such as transport, magnetism, electricity and optical limiting performance. For instance, the carbon nanomaterial prepared by Nasibulin *et al.* exhibit a low field threshold of about 0.65 V μm<sup>−1</sup> and a much higher current density compared with pure SWNTs.<sup>6a</sup> Additionally, the optical limiting performance of CNBs is found to be superior to that of SWNTs reported by Wang *et al.*<sup>9</sup> Although the above studies provided detailed investigation on the synthesis, configuration and physicochemical properties for CNBs, the experimental synthesis of CNBs is still limited and the commonly used CVD method also suffers its disadvantages, such as high operating temperature, toxic CO gas and specific reaction pressure, resulting in an inconvenient operation. Thus, it is necessary to explore new approach to synthesize CNBs with stable configuration, such as straightforward synthesis, convenient and environmental friendly process. RF (radio frequency) plasma treatment can be utilized as a novel alternative toward traditional CVD method to prepare CNBs by generating chemical active species. Virtually, all solid materials can be treated by this method with no solvent involved in the process, thus, producing no waste.<sup>10</sup> Meanwhile, previous reports have exhibited successful fabrication of CNTs anchored with various agents by this RF plasma treatment method.<sup>11</sup> Thus, in this study, we reported the synthesis of CNBs by RF plasma treatment for the first time as an easy operation, high efficient, economic and environmental benign process. Moreover, the C<sub>60</sub> fullerene-bonded-CNT is still referred to as CNBs due to its

<sup>a</sup>Institute of Plasma Physics, Chinese Academy of Sciences, P.O. Box 1126, Hefei 230031, P. R. China. E-mail: lijx@ipp.ac.cn; Tel: +86 65596617

<sup>b</sup>University of Science and Technology of China, Hefei, 230026, P. R. China

<sup>c</sup>Collaborative Innovation Center of Radiation Medicine of Jiangsu Higher Education Institutions, P. R. China

<sup>d</sup>NAAM Research Group, King Abdulaziz University, Jeddah, 21589, Saudi Arabia

<sup>e</sup>Department of Mathematics, Quaid-I-Azam University, Islamabad 44000, Pakistan

† Electronic supplementary information (ESI) available. See DOI: 10.1039/c7ra01530e

similar appearance with CNBs obtained by CVD method. Additionally, to better understand the benefit of RF plasma treatment method, a clearer explanation of the CVD method was given in ESI,<sup>†</sup> accompanying with a schematic presentation of CVD method.

Fig. 1 illustrates the schematic view of the experiment setup, which mainly consists of one three-necked, round-bottom flask with winding coils and a pulsed dc power supply (a whole schematic view of the experiment setup was shown in Fig. S2<sup>†</sup>). The plasma coil served as a high-voltage (HV) electrode and directly connected to the pulsed dc power supply. Firstly, a 1 : 1 ratio (by mass) of CNTs and fullerene ( $C_{60}$ ) were mixed and grinded, which were subsequently transferred to the round bottom flask. The HV pulsed dc power with 100 W was applied to the plasma coil until  $N_2$  vacuum degree of the glass flask reached a relative stable state of  $\sim 3.9$  Pa. The CNT/fullerene mixtures were treated under this condition for about 1 h before injecting 20 mL carbon disulphide ( $CS_2$ ) into the round bottom flask. Finally, the whole mixture was continuously stirred for  $\sim 24$  h under ambient temperature after which the sample was collected and washed several times with  $CS_2$  to remove the unreacted  $C_{60}$ . With no extra post-synthetic process, the purified sample was dried in a vacuum oven at  $60^\circ C$  for 12 h to obtain the desired CNBs.

The produced CNBs structure was confirmed by HRTEM and Raman spectroscopy. Since the inherent vibration of CNBs during the electron beam penetration process, it is challenging to obtain clear TEM images of CNBs, as shown in Fig. 2 for both CNTs and CNBs. CNTs with  $C_{60}$  of various sizes were presented and this observation is consistent with the previously reported results.<sup>6,7,12</sup> Fig. 2a and b clearly demonstrated a smooth surface of CNTs with a diameter of  $\sim 5$  nm. However, after RF plasma treatment, a rough surface of CNBs was observed (Fig. 2c and d), which can be attributed to the micro-etch formations by RF plasma treatment and the addition of  $C_{60}$  (the spherical dots) on the surface of CNTs. The diameter of single modified  $C_{60}$  is measured to be about 1 nm, 1/5 of the CNTs diameter. However, the distribution of modified  $C_{60}$  on the CNTs surface is not uniform, due to the destruction of  $C_{60}$  and the formation of fullerene dimers or oligomers under the plasma treatment. Moreover, RF treatment time was varied as 30 min and 120 min to investigate effect of treatment time on the density of the

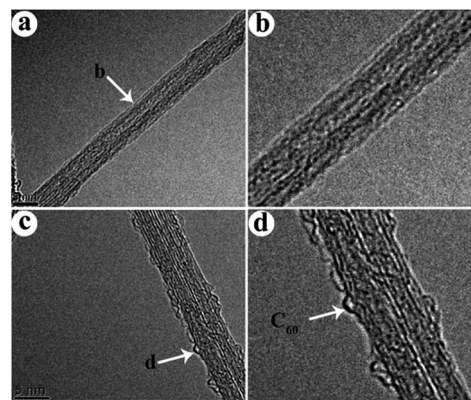


Fig. 2 (a) HRTEM image of CNTs after, (b) magnified image of (a), (c) HRTEM image of CNBs, (d) magnified image of (c).

buds. And the corresponding HRTEM images of CNBs were given in Fig. S4.<sup>†</sup> It can be seen that the RF treatment time has little effect on the density of the buds. In addition to varying the RF treatment time, impact of ratios of  $C_{60}$  : CNTs on the outcomes of the carbon structures was also investigated. Although it is fallacious to compare the outcomes of the carbon structures *via* varying the ratios of  $C_{60}$  : CNTs due to the uneven grind, it is still can be found that the density of buds increases with the increase of  $C_{60}$  : CNTs ratios from 0.5 to 2, shown in Fig. S5.<sup>†</sup> In spite of the density increase resulted from the higher mass ratio of  $C_{60}$  : CNTs, CNBs obtained from the ratio of 1 : 1 was still chosen to make the discussion considering the relative high density of buds and cost savings. Additionally, increasing the yield of CNBs is still under processing. Moreover, the raw CNTs and  $C_{60}$  fullerenes were exposed to the RF plasma treatment for 1 h. And the corresponding TEM images were given in Fig. S6 and S7,<sup>†</sup> respectively. It can be seen that the overall morphologies of CNTs did not change after RF plasma treatment except the appearance of rough surface due to the micro-etch formations resulted from the RF plasma treatment. Moreover, the plasma treatment can produce chemically active species on the surface of the substrate and have no effect on its inner structure, thus, plasma treatment does not lead to interesting surface structures. Without attaching to the CNTs surface, the  $C_{60}$  fullerenes after plasma treatment tend to agglomerate, since  $C_{60}$  fullerenes are known to be easily polymerized upon application of external energy sources, such as electron beams or photons.<sup>13</sup> And clusters of  $C_{60}$  fullerenes are clearly observed in an aggregated state (Fig. S7a<sup>†</sup>). Additionally, typical HRTEM image of the fullerene cluster is shown in Fig. S7b.<sup>†</sup> The images clearly show that the  $C_{60}$  fullerenes are polycrystalline in nature, which is supposedly most free from the confusion because of the projection of overlapping structures.<sup>14</sup>

To further corroborate the formation of CNBs structure, Raman spectra of CNBs were carried out, as shown in Fig. 3. The  $I_G/I_D$  ratio is  $\sim 9$ , indicating low defectiveness of the CNTs. The presence of this D band indicated the CNBs structure. Since even tiny bonded carbon from addition reaction can result in the intensity increase of D band, the covalent bonding of  $C_{60}$

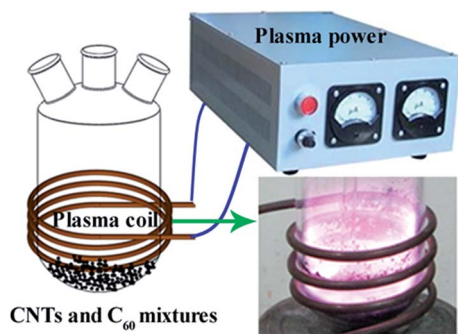


Fig. 1 Schematic view of the experiment setup.



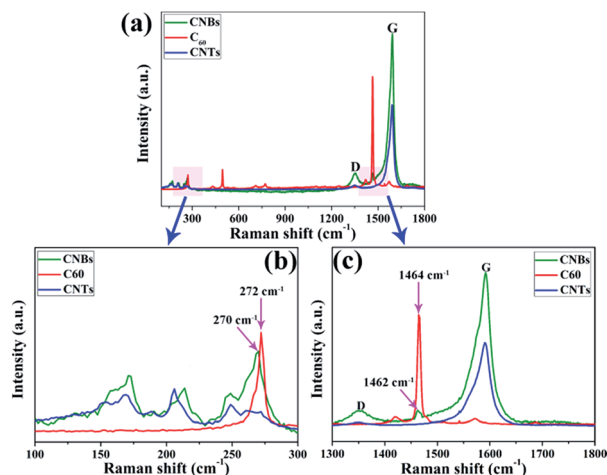


Fig. 3 (a) Raman spectrum of the CNBs,  $C_{60}$  and CNTs; (b) and (c) magnified Raman spectrum of the CNBs,  $C_{60}$  and CNTs in the range of 100–300  $\text{cm}^{-1}$  and 1300–1800  $\text{cm}^{-1}$ , respectively.

attached to the CNTs surface can account for this increase. It is well known that Raman active modes of  $C_{60}$  are measurable at ambient condition. However, vibrational modes of  $C_{60}$  in CNBs structure are difficult to detect due to the strong intensity of vibrational modes from CNTs. Thus, in this study, based on the previous reports,<sup>6c,15</sup> excitation energy of 2.33 eV was applied to detect the vibrational modes of  $C_{60}$  in CNBs structure. Clearly, it is significant to note that  $C_{60}$  fullerenes in the assembled structures showed a red-shift (softening) in their position. As shown in Fig. 3b, the  $H_g(1)$  mode of  $C_{60}$  fullerenes is red shifted from 272  $\text{cm}^{-1}$  to 270  $\text{cm}^{-1}$ . And the  $A_g(2)$  mode (pentagon pinch mode) of  $C_{60}$  fullerenes is red shifted from 1464  $\text{cm}^{-1}$  to 1462  $\text{cm}^{-1}$ , shown in Fig. 3c. These red shifts in the  $C_{60}$  modes are indicative of strong interaction between the two types of nano-building blocks within the assembled structure of CNBs. Similar result can also be found in previous report.<sup>16</sup> The simultaneous observation of vibrational modes of both  $C_{60}$  and CNTs clearly demonstrates the successful preparation of CNBs, which is consistent with result obtained from HRTEM (Fig. 2).

A possible mechanism was proposed to explain the formation of CNBs by RF plasma treatment. By treating with RF plasma,  $N_2$  can be excited as the active nitrogen species (*i.e.*  $N^*$ , shown in Fig. S8†).<sup>11a</sup> The *in situ* generated active nitrogen species (*i.e.*  $N^*$ ) can easily react with CNTs to form large amounts of active active [CNTs]\* because of its large surface area. Simultaneously, the active nitrogen species (*i.e.*  $N^*$ ) can also react with  $C_{60}$  to form  $[C_{60}]^*$ . Finally, the activated [CNTs]\* with active carbons can react with and  $C_{60}$  or  $[C_{60}]^*$  in liquid medium to form CNBs.<sup>17,18</sup> Additionally, the formation mechanism of CNBs is just anticipation, since it has no data to support it, and the precise formation mechanism of CNBs is still under processing. However, as previously reported,<sup>7,19,20</sup>  $C_{60}$  in CNBs would likely be damaged by the electron beam considering the limited free available carbon atoms provided by CNTs. To repair the damage of anchored  $C_{60}$  induced by the electron beam, weakly bonded carbon atoms are supposed to move to  $C_{60}$  over the surface of CNTs, during which the carbon atoms are very

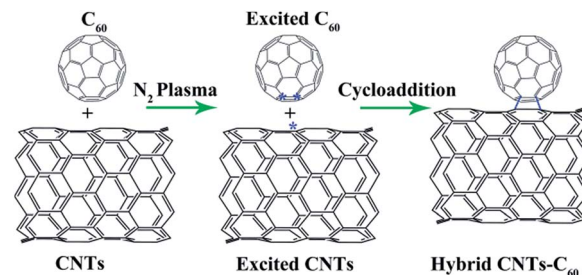


Fig. 4 Schematic presentation of the CNBs formation.

likely to be trapped due to large coverage of amorphous carbon structures on the outer surface of CNTs. During the RF plasma treatment, the  $T_p$  (plasma temperature) is within the range of  $2 \times 10^3$  to  $3 \times 10^4$  K,<sup>21</sup> which equals to beam energies of 0.2–3 eV, much lower than the  $C_{60}$  total bond energy (eV) of 419.75 eV.<sup>22</sup> Thus, it can be inferred that the  $C_{60}$  cannot be damaged during the RF plasma treatment. The defects caused by the electron beam from the TEM may also lead to the formation of CNBs. As discussed above, the formation of CNBs can be attributed to two aspects, being the cycloaddition between  $C_{60}$  and CNTs and the defects caused by the electrons generated during the TEM characterization. Fig. 4 provided a possible schematic depiction of the formation mechanism of CNBs through the cycloaddition between  $C_{60}$  and CNTs.

In summary, an efficient, economical and easy to operate method was developed for the successful synthesis of CNBs. The CNBs structure was confirmed by HRTEM in combination with Raman spectroscopy. The CNBs structures created here may be utilized as precursors in synthetic processes of nanotube junctions which can be further applied to composite and electronic fields. Additionally, since current CNBs form a relatively small percentage of CNTs, the scale-up of the production of CNBs is under investigation, to demonstrate the robustness of this new technique.

## Acknowledgements

We are grateful for financial support from the National Natural Science Foundation of China (21272236, 21677146, U1530131). The Jiangsu Provincial Key Laboratory of Radiation Medicine and Protection and the Priority Academic Program Development of Jiangsu Higher Education Institutions are also acknowledged.

## Notes and references

- (a) J. I. Choi, H. S. Kim, H. S. Kim, G. I. Lee, J. K. Kang and Y. H. Kim, *Nanoscale*, 2016, **8**, 2343–2349; (b) A. V. Talyzin, I. V. Anoshkin, A. V. Krashennnikov, R. M. Nieminen, A. G. Nasibulin, H. Jiang and E. I. Kauppinen, *Nano Lett.*, 2011, **11**, 4352–4356; (c) A. Chuvilin, E. Bichoutskaia, M. C. Gimenez-Lopez, T. W. Chamberlain, G. A. Rance, N. Kuganathan, J. Biskupek, U. Kaiser and A. N. Khlobystov, *Nat. Mater.*, 2011, **10**, 687–692; (d) Y. G. Li, W. Zhou, H. L. Wang, L. M. Xie, Y. Y. Liang,



- 1 F. Wei, J. C. Idrobo, S. J. Pennycook and H. J. Dai, *Nat. Nanotechnol.*, 2012, **7**, 394–400.
- 2 B. W. Smith, M. Monthieux and D. E. Luzzi, *Nature*, 1998, **396**, 323–324.
- 3 S. B. Chikkannanavar and D. E. Luzzi, *Nano Lett.*, 2005, **5**, 151–155.
- 4 H. J. Shen, *Mater. Lett.*, 2007, **61**, 527–530.
- 5 M. Vizueté, M. Barrejón, M. J. Gómez-Escalónilla and F. Langa, *Nanoscale*, 2012, **4**, 4370–4381.
- 6 (a) A. G. Nasibulin, P. V. Pikhitsa, H. Jiang, D. P. Brown, A. V. Krashennnikov, A. S. Anisimov, P. Queipo, A. Moisala, D. Gonzalez, G. Lientschnig, A. Hassanien, S. D. Shandakov, G. Lolli, D. E. Resaco, M. Chol, D. Tománek and E. I. Kauppinen, *Nat. Nanotechnol.*, 2007, **2**, 156–161; (b) A. G. Nasibulin, A. S. Anisimov, P. V. Pikhitsa, H. Jiang, D. P. Brown, M. Choi and E. I. Kauppinen, *Chem. Phys. Lett.*, 2007, **446**, 109–114; (c) Y. Tian, D. Chassaing, A. G. Nasibulin, P. Ayala, H. Jiang, A. S. Anisimov and E. I. Kauppinen, *J. Am. Chem. Soc.*, 2008, **130**, 7188–7189.
- 7 R. J. Nicholls, J. Britton, S. S. Meysami, A. A. Koós and N. Grobert, *Chem. Commun.*, 2013, **49**, 10956–10958.
- 8 (a) A. Sarmah and R. K. Roy, *Chem. Phys.*, 2016, **472**, 218–228; (b) X. Wu and X. C. Zeng, *Nano Lett.*, 2009, **9**, 250–256; (c) H. Y. He and B. C. Pan, *J. Phys. Chem. C*, 2009, **113**, 20822–20826; (d) A. Seif, E. Zahedi and T. S. Ahmadi, *Eur. Phys. J. B*, 2011, **82**, 147–152; (e) J. Raula, M. Makowska, J. Lahtinen, A. Sillanpää, N. Runeberg, J. Tarus, M. Heino, E. T. Seppälä, H. Jiang and E. I. Kauppinen, *Chem. Mater.*, 2010, **22**, 4347–4349.
- 9 J. Wang, K. S. Liao, D. Früchtel, Y. Tian, A. Gilchrist, N. J. Alley, E. Andreoli, B. Aitchison, A. G. Nasibulin, H. J. Byrne, E. I. Kauppinen, L. Zhang, W. J. Blau and S. A. Curran, *Mater. Chem. Phys.*, 2012, **133**, 992–997.
- 10 B. Akhavan, K. Jarvis and P. Majewski, *ACS Appl. Mater. Interfaces*, 2015, **7**, 4265–4274.
- 11 (a) D. D. Shao, J. Hu and X. K. Wang, *Plasma Processes Polym.*, 2010, **7**, 977–985; (b) D. Shao, J. Hu, C. L. Chen, G. D. Sheng, X. M. Ren and X. K. Wang, *J. Phys. Chem. C*, 2010, **114**, 21524–21530.
- 12 Y. Tian, D. Chassaing, A. G. Nasibulin, P. Ayala, H. Jiang, A. S. Anisimov, A. Hassanien and E. I. Kauppinen, *Phys. Status Solidi B*, 2008, **245**, 2047–2050.
- 13 (a) J. H. Yao, Y. J. Zou, X. W. Zhang and G. H. Chen, *Thin Solid Films*, 1997, **305**, 22–25; (b) S. G. Wang, E. K. Tian and C. W. Lung, *J. Phys. Chem. Solids*, 2000, **61**, 1295–1300; (c) J. Zhang, F. Ma and K. Xu, *Appl. Surf. Sci.*, 2004, **229**, 34–42.
- 14 H. S. Shin, S. M. Yoon, Q. Tang, B. Chon, T. Joo and H. C. Choi, *Angew. Chem.*, 2008, **120**, 705–708.
- 15 (a) T. Pichler, H. Kuzmany, H. Kataura and Y. Achiba, *Phys. Rev. Lett.*, 2001, **87**, 267401; (b) R. Pfeiffer, H. Kuzmany, W. Plank, T. Pichler, H. Kataura and Y. Achiba, *Diamond Relat. Mater.*, 2002, **11**, 957–960; (c) P. M. Rafailov, C. Thomsen and H. Kataura, *Phys. Rev. B: Condens. Matter Phys.*, 2003, **68**, 193411.
- 16 M. S. Amer and J. D. Busbee, *J. Phys. Chem. C*, 2011, **115**, 10483–10488.
- 17 A. Hirsch, *Synthesis*, 1995, 895–913.
- 18 (a) M. Ueda, T. Sakaguchi, M. Hayama, T. Nakagawa, Y. Matsuo, A. Munechika, S. Yoshida, H. Yasudad and I. Ryu, *Chem. Commun.*, 2016, **52**, 13175–13178; (b) S. Yano, M. Naemura, A. Toshimitsu, M. Akiyama, A. Ikeda, J. Kikuchi, X. D. Shen, Q. Duan, A. Narumi, M. Inoue, K. Ohkubo and S. Fukuzumi, *Chem. Commun.*, 2015, **51**, 16605–16608.
- 19 T. Füller and F. Banhart, *Chem. Phys. Lett.*, 1996, **254**, 372–378.
- 20 F. Ding, Z. Xu, B. I. Yakobson, R. J. Young, I. A. Kinloch, S. Chu, L. Deng, P. Puech and M. Monthieux, *Phys. Rev. B: Condens. Matter Mater. Phys.*, 2010, **82**, 041403.
- 21 H. Huang and L. Tang, *Energy Convers. Manage.*, 2007, **48**, 1331–1337.
- 22 D. R. Lide, *CRC Handbook of Chemistry and Physics*, CRC Press, Taylor & Francis, Boca Raton, 86th edn, 2005, pp. 5–42.

